Techno-economic Feasibility Analysis of Solar Photovoltaic Power Generation for Buildings

Article *in* Applied Thermal Engineering · August 2016

DOI: 10.1016/j.applthermaleng.2016.07.199

Applied Thermal Engineering 108 (2016) 1362–1371

Contents lists available at ScienceDirect

Applied Thermal Engineering

journal homepage: www.elsevier.com/locate/apthermeng

Research Paper

Techno-economic feasibility analysis of solar photovoltaic power generation for buildings

Xiongwen Zhang *, Menyu Li, Yuanfei Ge, Guojun Li

MOE Key Laboratory of Thermo-Fluid Science and Engineering, Xi'an Jiaotong University, Shaanxi 710049, China

HIGHLIGHTS

- A model for optimal component sizes of hybrid energy system (HES) is presented.
- The techno-economic feasibility of PV for building in context of China is studied.
- The use of PV reduces COE by 46% for customers in the commercial building.
- The use of PV increases COE by 9.55% for customers in the residential building.

ARTICLE INFO

Article history:
Received 6 April 2016
Revised 19 July 2016
Accepted 31 July 2016
Available online 5 August 2016

Keywords:
Hybrid energy systems
Building added photovoltaics
Techno-economic assessment
Component sizing

ABSTRACT

The Building Added PV (BAPV) plays an important role for developing green buildings. This work conducts a techno-economic feasibility study of BAPV for commercial and residential building hybrid energy systems (HES). A component sizing model based on the optimal power dispatch simulations with the objective of minimum cost of energy (COE) is used to determine the component sizes of HES. The techno-economic performances of two HES composed of BAPV and batteries for residential and commercial buildings are investigated. The results show that the use of BAPV in the commercial building HES can reduce the electricity bill for customers owing to the government subsidies on PV as well as due to the similar characteristics of the load profile as to the solar radiation profile. However, due to temporal dislocation between the load and solar radiation patterns, the use of PV in the residential building HES may significantly increase the initial capital cost and replacement cost of battery, resulting in the COE of the residential building HES with BAPV even higher than the residential electricity price. The techno-economic performances of battery (e.g., the lifetime and capital cost) have more effect on the COE of the residential building HES than that of PV.

1. Introduction

Solar energy is a renewable and clean energy resource. It will almost certainly play an increasingly important role in the future energy network [1]. The use of solar energy in the buildings has become the most popular choice in the development of green buildings or even zero emission buildings with a fully photovoltaic (PV) power system. On the other hand, due to the fluctuation and intermittence of the solar source, PV is generally required to be combined with other distributed energy resources (DERs), such as batteries, diesel generators, fuel cells, and microturbines. These DERs and the loads can be integrated together and managed by a hybrid energy system (HES). The use of HES technology provides the opportunity of integrating the Building Added PV (BAPV) in the main grid.

The component sizing is believed to have significant effect on the performances of the HES. For a specific load profile, the deliverable power source has to be enough to meet the power demands in the operation period. The optimal sizes for battery and PV in a HES are highly dependent on the characteristics of load profile, which correspondingly affect the economic feasibility of integrating the PV in the HES. It is known that the differences of the load profiles between the residential and commercial buildings are significant. The economic performances of deploying BAPV HES vary greatly between the residential and commercial applications, which correspondingly affect the optimal components sizing for the BAPV HES.

The system components sizing is actually an optimization process. Its target is to find the optimal-size combination of the system components that can reliably supply electric power to a

* Corresponding author.
E-mail address: xwenz@mail.xjtu.edu.cn (X. Zhang).

http://dx.doi.org/10.1016/j.applthermaleng.2016.07.199
1359-4311/

Nomenclature

BoP	balance of plant
$c_{PV_a}^{cap}$	capital cost of PV per square meter (¥ m^{-2})
$c_{PV_p}^{cap}$	capital cost of PV per kW_p (¥ kW_p^{-1})
C^{dep}	capital depreciation cost (¥ h^{-1})
C^{fue}	fuel cost (¥ kg^{-1})
C^{dam}	emissions damage cost (¥ kg^{-1})
C_{SYS}^{mai}	system maintenance cost (¥ h^{-1})
C_{BoP}^{dep}	capital depreciation cost of system balance of plants (BoPs) (¥ h^{-1})
C_{phy}^{dep}	capital depreciation cost based on physical lifetime (¥ h^{-1})
C_{run}^{dep}	capital depreciation cost based on the lifetime throughput (¥ h^{-1})
C_{pool}	candidates of sampling population pool
COE	cost of energy (¥ kW h^{-1})
d	load demand (kW)
DER	distributed energy resource
f^{emi}	emissions factor of DERs (kg kJ^{-1})
$f_{CO_2}^{emi}$	emissions factor of CO_2 (kg kJ^{-1})
M	number of the discretized time interval
N	number of DERs
N_p	number of populations in C_{pool}
N_u	number of the increased populations
p	energy delivered by the DERs (kW h)
P_{life}	energy lifetime throughput with DERs (kW h)
PV	photovoltaic
R_p	the peak of solar radiation (kW m^{-2})
t_{cont}	hours that the battery continually supplies to the maximum load demand (h)
SOC	state of charge
T	end of simulation time (h)
T_0	start of simulation time (h)
Δt	time interval (h)
t	lifetime of DERs (h)
U	unit conversion factor (kW m^{-2})
w	size of DERs (the units for DG, BT and PV are kW, kW h and m^2, respectively)
W_{range}	size range of DERs
C_{pool}	candidates of sampling population pool
N_p	the number of populations in C_{pool}
N_u	the number of the increased populations
p	operation setting
I	the number of iterations
W_{space}	sizing space for DERs (the units for DG, BT and PV are kW, kW h and m^2, respectively)

Greek letters

η	operating efficiency of DERs

Subscripts

i	index of DERs
k	index of the discretized time interval
p	peak
phy	physical
run	running
SYS	system

Superscript

dam	damage
dep	depreciation
emi	emission
fue	fuel
mai	maintenance
max	maximum
min	minimum

given demand profile with the lowest cost of energy (COE) [2]. Traditional approach for sizing the hybrid energy system employs rule-of-thumb methods that are based on hardware expertise knowledge and experiences of the respective designers [3]. Obviously, it is difficult to get the optimal design solution simply by using such rule-of-thumb methods due to the complexity of the problem (e.g. grid-interaction [4,5]) and the highly nonlinear characteristics of the components in the HES [6,7]. The special optimization method is required for the techno-economic assessment of the energy system. There are a few software programs including HYBRID2, DER-CAM, HOMER, RETScreen and HOGA, etc. used for the assessment of techno-economic performances for the HES [7–15]. In these software tools, DER-CAM is particularly applied to the power dispatch operation of pre-defined HES while HYBRID2 and RETScreen are applied in system detail designs and project techno-economic feasibility studies, respectively. The criteria of optimization algorithm may differ according to each application concerned. Mostly, the optimal component sizing algorithms are developed based on the minimization of the cost and deficiency of the power supplies [16–19]. There is the case that the so-called sustainability is taken as a criterion in the optimization objective [20]. In practical operation, the lifetime of some components (e.g. batteries) is highly dependent on the ~~on/off/~~current flow intensity. Zhang et al. [2] has developed a new economic model taking into account the capital depreciation cost of components in the COE evaluation. Another important issue is the optimization technique used for the techno-economic analysis of the HES. Many researchers have investigated different optimization algorithms [21], such as genetic algorithm [22–25], particle swarm optimization [26–28], linear programming [2,29,30], neural networks [31,32], simplex algorithm [33], and iterative and probabilistic approaches [34–36].

The solar PV is one of the most promising renewable energy technologies to produce electricity on site without concerns of energy supply and environmental harm. Interest in the building integration of PV is growing worldwide. However, the economic performance of deploying solar PV in different buildings has significant distinctions. The economic feasibility of using solar PV in the system has to be evaluated before the project implementation. Actually, it is strongly related with the characteristics of load profile. The discrepancies of load profiles between different types of building applications, e.g. the commercial buildings and residential buildings, are significant. For a PV integrated system, the size of energy storage component is strongly dependent on the matching degree between the load profile and the solar radiation profile, which gives significant effect on the COE of system. This work presents a techno-economic assessment of the BAPV integrated HES at Xi'an, China. The economic feasibility of BAPV for commercial and residential building HES is evaluated by conducting the model simulations with the approach of Ref. [2]. In Ref. [2], a new approach based on the power dispatch simulations has been developed for the techno-economic assessment of HES. In this model, the optimal size combination of the HES components is achieved by minimizing the COE with consideration to the capital depreciation cost, fuel cost, emission damage cost and maintenance cost.

2. Mathematical approach

Proton exchange membrane fuel cells (PEMFCs) are power generator fueled by hydrogen. PEMFC is a type of clean technology for power generation. It contains many advantages, such as low operating temperature, high efficiency, and light and compact, which make them ideal for stationary power generation applications in buildings. This work considers PEMFC in the building hybrid systems. A HES composed of BAPV, battery, and PEMFC is studied in this work. In this system, the DC distributed energy resources (DERs) are integrated by a DC bus and is connected to the main grid and load through a bi-directional electronic converter. In the HES operation, the deliverable power from DERs is required to fully cover the power demand in the given time range. In this case, the component size combinations highly depend on the characteristics of the load profile and solar radiation profile that are closely related with the type of building application and the location.

The COE is calculated from the summation of the capital depreciation cost (C^{dep}), fuel cost (C^{fue}), emissions damage cost (C^{dam}), and system maintenance cost (C^{mai}_{SYS}) in terms of the per kW h energy provided to the load demand during the time [T_0, T]. The cost calculation is based on the nominal cash flow. The mathematical formation of COE can be written as follows:

$$COE = \frac{\sum_{k=1}^{M}\sum_{i=1}^{M}\left(C^{dep}_{i,k} + C^{fue}_{i,k} + C^{dam}_{i,k}\right) + C^{dep}_{BoP} + C^{mai}_{SYS}}{\sum_{k=1}^{M} d_k} \tag{1}$$

The number of the discretized time interval (M) is given by

$$M = \frac{T - T_0}{\Delta t} \tag{2}$$

Within the time interval Δt, the capital depreciation cost based on physical lifetime for a component is calculated by

$$C^{dep}_{phy} = \Delta t \frac{wc^{cap}}{t_{phy}} \tag{3}$$

For a specific DER, the capital depreciation cost based on the lifetime throughput is given as

$$C^{dep}_{run} = p\frac{wc^{cap}}{P_{life}} \tag{4}$$

The specific cost of PV based on per square meter is obtained by

$$c^{cap}_{PV_a} = c^{cap}_{PV_p} U \tag{5}$$

The value of U equals the efficiency of the PV. The capital depreciation costs for DERs are equal to the higher value of C^{dep}_{phy} and C^{dep}_{run} as:

$$C^{dep} = \max\left(C^{dep}_{phy}, C^{dep}_{run}\right) \tag{6}$$

The BoPs sizes are designed according to the maximum value of load profile. The capital depreciation cost of BoPs is considered to be independent of the system operation control settings. This can be estimated based on the component physical lifetime as given by Eq. (3). It is noted that the inverters for PV are considered as the components of BoPs. The system maintenance cost C^{mai} in the present model only considers the manpower cost, which is decided according to the average load demand and the salary standard of the places. The DER fuel cost C^{fue} is determined by

$$C^{fue} = p\frac{c^{fue}}{q_v \eta} \tag{7}$$

In this work, only PEMFC has the hydrogen fuel cost. The emission damage cost represents the cost of emitting harmful gases that have damaging effects to ecosystems, affecting health and possibly leading to the loss of human life. It is estimated based on the overall cost of controlling the release or cleanup of the emissions. In this work, we take into account only the emission of CO_2 in the economic model. The damage cost of CO_2 used in this study is set to be 0.1637 ¥/kg according to Ref. [37]. The damage cost for CO_2 emission of DERs within time interval Δt is calculated as follows:

$$C^{dam} = 3600p\frac{f^{emi}_{CO_2} c^{dam}_{CO_2}}{\eta} \tag{8}$$

Combining Eqs. (3) to (8), the objective function of the optimization problem can be formulated as follows:

$$\min\left\{\sum_{k=1}^{M}\sum_{i=1}^{N}\left[\max\left(\Delta t\frac{w_i c^{cap}_i}{t^{phy}_i}, p_{i,k}\frac{w_i c^{cap}_i}{P^{life}_i}\right) + p_{i,k}\frac{c^{fue}_i}{q_i\eta_i} + 3600p_{i,k}\frac{f^{emi}_{CO_2,i}c^{dam}_{CO_2,i}}{\eta_i}\right]\right\} \tag{9}$$

The constraints for the objective function Eq. (9) are given as follows [2]:

$$\sum_{i=1}^{N} P_{i,k} = d_k \text{ where } k = 1,\ldots,M \tag{10}$$

$$\begin{cases} \max\left(-V^{ch\arg e}_i I^{ch\arg e}_{MAX,i}\Delta t, -\frac{w_i}{\eta^{ch\arg e}_i}\right) \leqslant p_{i,k} < 0 \\ \quad \text{for charge process of battery} \\ 0 \leqslant p_{i,k} \leqslant \min\left(V^{disch\arg e}_i I^{disch\arg e}_{MAX,i}\Delta t, w_i\eta^{disch\arg e}_i\right) \\ \quad \text{for discharge process of battery} \\ 0 \leqslant p_{i,k} \leqslant \eta_i R_k w_i \Delta\, t \text{ for PV} \\ 0 \leqslant p_{i,k} \leqslant w_i \Delta t \quad \text{for PEMFC} \end{cases} \tag{11}$$

$$\begin{cases} 0 \leqslant SOC_{i,k} = SOC_{i,k-1} + \frac{p_{i,k}}{\eta^{disch\arg e}_i w_i} \leqslant 1 \quad \text{for } p_{i,k} > 0 \\ 0 \leqslant SOC_{i,k} = SOC_{i,k-1} + \frac{\eta^{ch\arg e}_i p_{i,k}}{w_i} \leqslant 1 \quad \text{for } p_{i,k} \leqslant 0 \end{cases} \tag{12}$$

Thus, the sizing optimization problem is to obtain w by solving the objective function Eq. (9) with the constraint conditions Eqs. (10)–(12). Fig. 1 shows the flowchart for solving the optimization formulation of Eqs. (9)–(12). The main loop from *Start* to *End* is to find the decision variable w with the lowest COE using a so-called random search method [26]. The randomized optimization technique follows the processes as:

Step 1: Randomly generate a candidate of DERs size combination w within the specified size spaces.
Step 2: With regards to the generated w, the simulated optimal operation settings are decided by solving the optimization model Eqs. (10)–(12).
Step 3: The system COE is evaluated with Eq. (1) based on the DERs sizes w and the corresponding operation settings p. Then, the random DERs sizes w are added to the population pool C_{pool} and t the elements of pool population is sorted according to the COE value.
Step 4: The spaces of DERs sizes are updated as the number of the increased population reaches N_u. This step can accelerate the convergence of the random search process to the optimal solutions. The candidate from C_{pool} with the lowest COE is chosen as the final solution when the number of the generated random w reaches the pre-specified maximum. Otherwise, the algorithm process returns to Step 1.

The detail for randomized optimization technique is referred to [2].

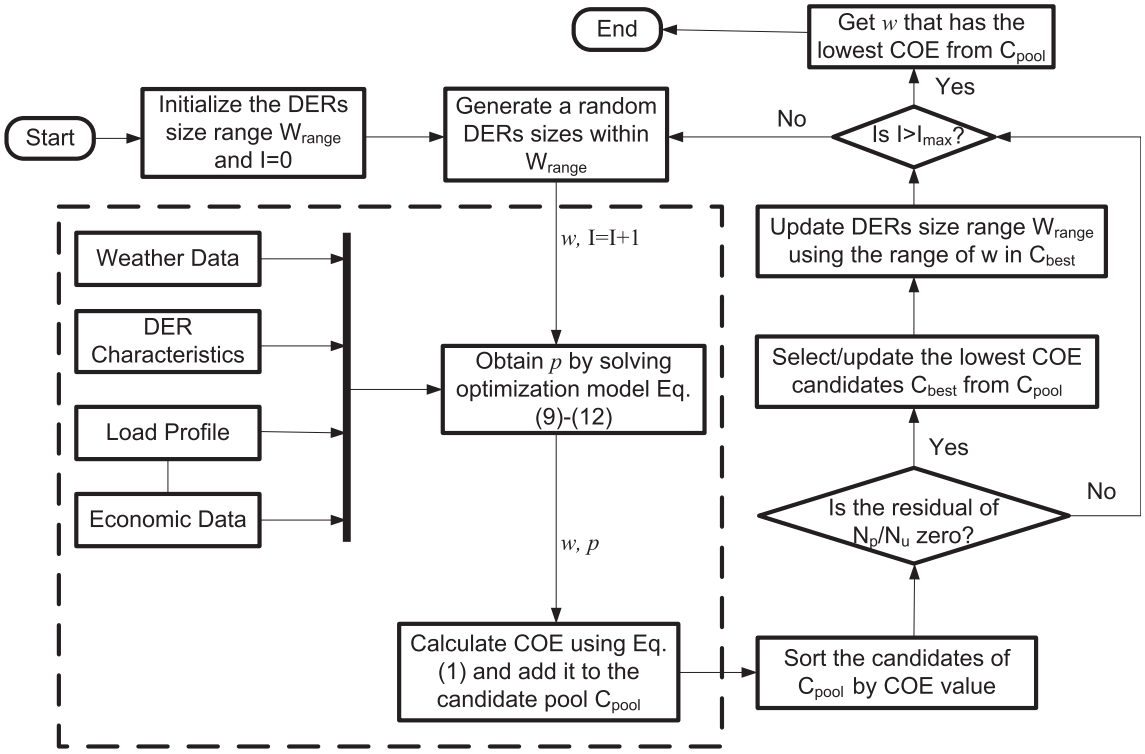

Fig. 1. The flowchart of components sizing algorithm for the HES.

3. Input specifications

The buildings considered in this work are located at Xi'an, approximately the geographic center of China. The position of Xi'an is 34.34°N and 108.94°E. A commercial office block (10,000 m^2) and an independent villa are selected as the case study. Fig. 2(a) shows the measured daily load profile for a typical office building [38]. Comparatively, the power demand of the office building is stable. In the daytime on work, the demand is approximately 550 kW while it is 80 kW in the night. The typical daily load profile for the villa is estimated from Refs. [39,40]. As shown in Fig. 2(b), the daily load profile for the villa presents unsteady. The peak of power demand appears between 7:00 PM and 8: 00 PM when it is sundown and dinner time in the summer at Xi'an. The components size of the HES is determined based on the weekly power dispatch simulation using the mathematical approach proposed in Section 2. Based on the daily load profiles, the weekly simulated load profiles can be generated via the stochastic process for the office building and villa. The random magnitude for the stochastic process is 20%.

The power output of BAPV is strongly dependent on the solar radiation profile. Fig. 3 shows a typical weekly solar radiation profile of Xi'an, China, which is generated by a stochastic reconstruction model based on the measured data [41]. This model can reconstruct the solar radiation profile with the only input of the cloud condition of the sky (i.e., fair, partly cloudy, overcast, and rain/snow, etc.). The accuracy of the solar radiation reconstruction model can achieve the normalized root mean square error on average 23.4% and 7.2% for the one-minute temporal resolution and hourly integral values, respectively. The weekly solar radiation profile covers all weather categories including the fair, partly cloudy, cloudy, and rain, enabling the solutions of the optimization process applicable to all weather conditions. The technical data employed in the computations for components sizing optimization are given in Table 1. It is noted that the cost is computed in Chinese Yuan (CNY). The current exchange rate of US dollar (USD) to CNY is 6.35. The subsidies for PV generation is 0.42 ¥/kW h. The BoPs cost includes the replacement cost of components during the lifetime of system. Besides the load variation, the variations for other cost related parameters (e.g., fuel cost, electricity price, discount rate, emission damage cost, etc.) are not considered in the model. The computations are implemented with the software platform MATLAB 7.14.

4. Results and discussion

4.1. Optimization results

Fig. 4 shows the convergences of the optimization process in the component sizing of HES for both the residential and commercial buildings. The points in Fig. 4 represent the size combination of three components (the main grid, PV and battery) for the HES. It can be seen from Fig. 4 that the COE goes down along the direction of the arrow. Note that the direction of the arrow also shows the convergence direction in the optimization computations. The higher is the COE, the less is the number of the points. This is because the optimization algorithm excludes the areas with higher COE value at the beginning of the optimization process. As shown in Fig. 4, the search space is contracted along the direction of arrow with the growth in the number of calculations. In areas with possible optimal solutions, a more intensive search is conducted, causing the value of COE to approach the minimum. It indicates that the optimization approach can effectively enable the search space converge to the field with low COE. The lowest COEs for the commercial and residential building HES are given to be 0.6982 ¥/kW h and 0.5459 ¥/kW h, respectively. Due to the high cost of PEMFC and hydrogen, the optimization process excludes the use of PEMFC in both HES.

The COE for the optimal size combination of commercial building HES is approximately 30% higher than that of the residential

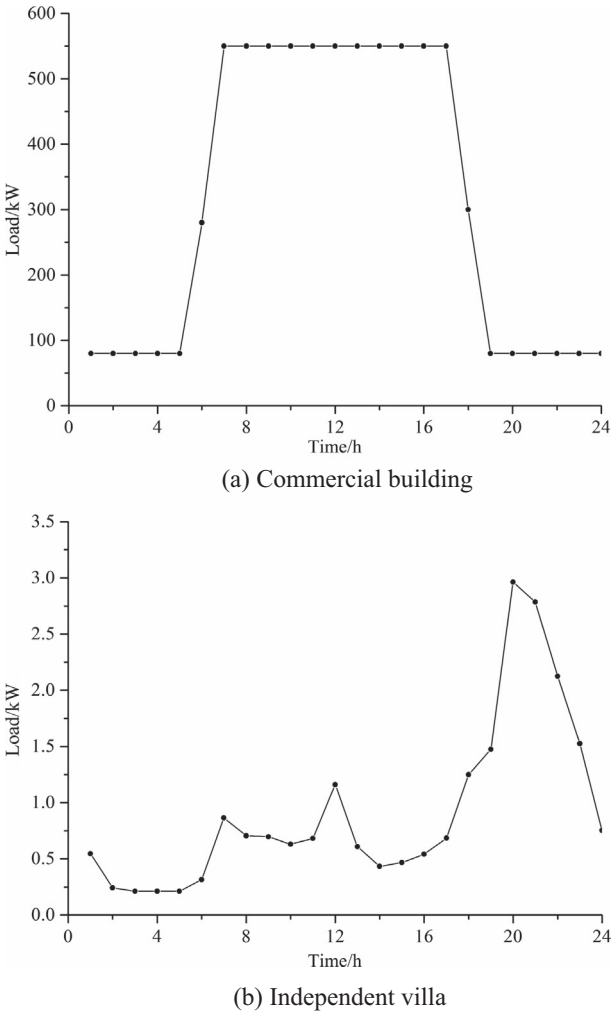

Fig. 2. Typical daily load profiles for the commercial office building and independent villa.

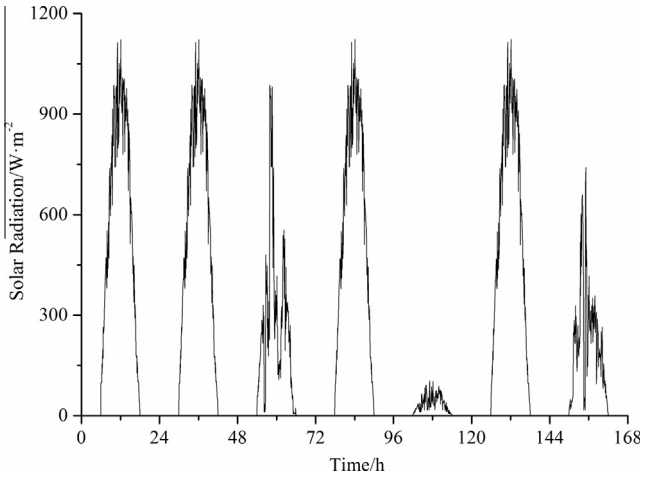

Fig. 3. The weekly solar radiation profile.

building HES. This is because the electricity price for the commercial building is higher than that of the residential building. It can be seen from Fig. 4(a) that the low COE for the HES of commercial building locates in the area with larger capacities of BAPV. On the contrary, the low COE for the residential building HES locates

Table 1
Technical data for components sizing optimization.

Name	Symbol	Value	Source
PEMFC			
Capital cost	c_{PEM}^{cap}	11,408 ¥/kW	[42]
Fuel cost	c^{fue}	51.43 ¥/kg	*e*
Efficiency	η_{PEM}	60%	[43]
Physical lifetime (working time)	t_{phy}	15 Years	*a*
Main grid			
Capital cost	c_{Grid}^{cap}	0	*e*
Electricity price	$c^{electric}$	Commercial building: 1.2893 ¥/kW h Residential building: 0.4983 ¥/kW h	[44]
Coal consumption	C^{coal}	0.333 kg/kW h	[45]
Emission factor of coal	f^{coal}	0.68 t/tce	[46]
Emission damage cost of CO_2	$c_{\mathrm{CO^2}}^{dam}$	0.1637 ¥/kg	[37]
PV			
Capital cost	c_{PV}^{cap}	433 ¥/m^2	*e*
Efficiency	η^{PV}	17.12%	*e*
Physical lifetime (working time)	t_{phy}	20 Years	*a*
Subsidy of PV power generation		0.42 ¥/kW h	[47]
Battery[a]			
Capital cost	$c_{\mathrm{Battery}}^{cap}$	666.67 ¥/kW h	*e*
Charge-discharge cycle		600 Times	*e*
Physical lifetime (working time)	t_{phy}	5 Years	*e*
Maximal charge current	$I_{\mathrm{MAX},i}^{\mathrm{charge}}$	0.3 C	*a*
Maximal discharge current	$I_{\mathrm{MAX},i}^{\mathrm{discharge}}$	3 C	*a*
Charge efficiency	$\eta_{\mathrm{Battery}}^{\mathrm{charge}}$	90%	*a*
Maximal depth of discharge		40%	*s*
Discharge efficiency	$\eta_{\mathrm{Battery}}^{\mathrm{discharge}}$	90%	*a*
Others			
Loading variation		20%	*s*
System maintenance cost	C_{SYS}^{mai}	0.093 ¥/h	[2]
Balance-of-plant cost	C_{dep}^{BoP}	30% of initial capital cost	[6]
System lifetime	T_{phy}	15 Years	*a*

Note: *a*-assumed values, *e*-estimated values, *s*-specified values.
[a] Battery technology is referred to the valve regulated lead-acid battery from VISION GROUP, CHINA.

in the area with smaller capacities of BAPV. This is because that the commercial electricity price is so expensive (1.2893 ¥/kW h), which is even higher than the electricity cost of PV when the government subsidy is included in the economic model. Therefore, a large percentage of PV power generation causes low COE for the commercial building HES. However, as the big size of PV will increase the cost of energy storage, i.e. the battery cost, there is a balance. For the residential application, the price of electricity generated from the main grid is still cheaper than that from PV. From the point of view of reducing COE, a less PV used in the system is the choice to achieve the optimal solution.

Table 2 gives the results of the optimal size combination for both the residential and commercial building HES. Both results are obtained under the condition that the minimum percentage of the renewable energy source is 30%. As shown in Table 2, the BAPV-based HES for commercial building reduces the energy costs from 1.2893 ¥/kW h to 0.6982 ¥/kW h, giving approximately 46% cost savings for customers. However, deploying a BAPV-based HES in the residential building cannot reduce the energy bills for customers. The government needs to further increase the subsidy of PV power generation for the residential applications.

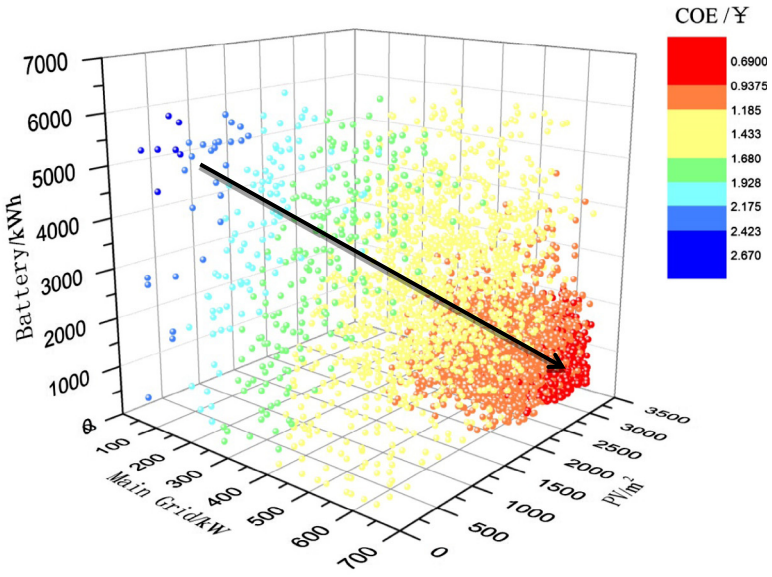

(a) Commercial building HES

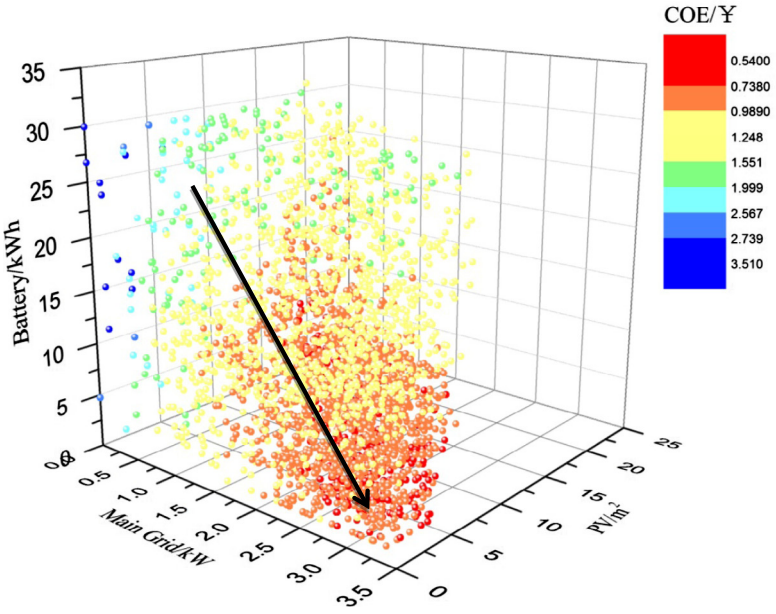

(b) Residential building HES

Fig. 4. The dependence of COE on the component sizes of residential and commercial building HES.

Table 2
Optimization results of the components sizes for residential/commercial building HES.

Components type	Main grid	PV	Battery	COE	Grid electricity price
Unit	kW	m^2	kW h	¥/kW h	¥/kW h
Case 1 Commercial building	629	3372	302	0.6982	1.2893
Case 2 Residential building	2.17	7.45	5.16	0.5459	0.4983

4.2. Techno-economic performances of commercial building HES

The optimal solution for the component sizes of commercial building HES is given as follows: main grid 629 kW (maximum power), PV 3372 m^2, and battery 302 kW h. In the following section, the techno-economic performances on this solution are presented.

Fig. 5 shows the weekly power dispatch of the DERs and main grid for the commercial building HES. The horizontal axis represents the time (hours) and the vertical axis represents the electricity required from the energy sources of hybrid energy system to meet the loads (kW). The negative values of the output from battery represent the charging process. Correspondingly, the positive

values of the output from battery represent the discharging process.

As seen from Fig. 5, the PV and main grid supply all energy to meet the load demand, where the PV provides the primary energy source for the electricity generation during daytime and the main grid is the main energy source in the night. In fair days (the 1st, 2nd, 4th and 6th day) as shown in Fig. 5, PV can provide adequate and stable power for the load requirement. When the electricity generated from PV is more than the demand of loads, the excess power is stored in the battery. In contrast, when PV cannot provide sufficient electricity to meet the load demand, the main grid will play the role to complement the electricity. Therefore, a typical power dispatch schedule at fair days is that the electricity is mainly generated from PV and is supplemented by the main grid in the mornings and evenings or at other special period of time. When days are cloudy or rainy (the 3rd and 7th day), the electricity generated from PV is no longer stable and gravely insufficient. In this case, the electricity is mainly supplied by the main grid to supplement the shortage of the PV power generation. Particularly as we can see from Fig. 5, as the 5th day is rainy weather, PV can only provide a very small part of the electricity and therefore the main grid supplies the most part of electricity. From Fig. 5, the sum of the electricity from main grid, PV and battery basically equals to the load, which is agreement to the energy balance set by constraints.

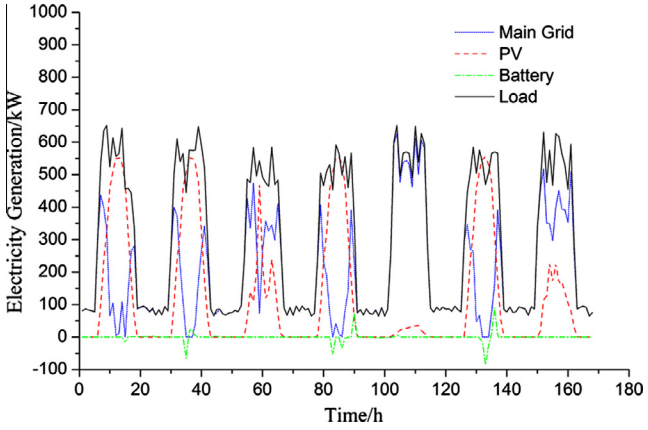

Fig. 5. The power dispatch schedule for the energy sources of the commercial building HES composed of 3372 m^2 PV and 302 kW h battery with grid connection (COE = 0.6982 ¥/kW h).

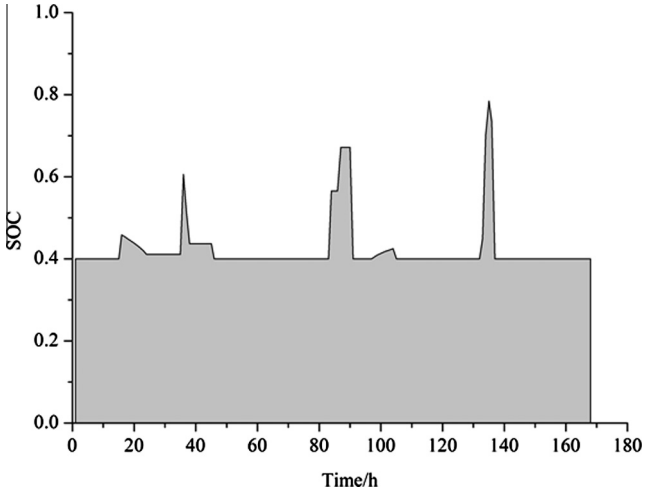

Fig. 6. The SOC of battery in the operation of the commercial building HES (COE = 0.6982 ¥/kW h).

It can be seen from Fig. 5 that the battery is less used in the case of commercial building HES. There is occasionally the excess electricity generated from PV being stored in the battery in fair days. For cloudy or rainy days, the HES directly uses the main grid to meet the loads demand. Fig. 6 illustrates the changes of the state-of-charge (SOC) of battery for the commercial building HES with the sizes of 3372 m^2 PV and 302 kW h battery. As shown in Fig. 6, the maximum SOC of battery achieves approximately 80% at noontime in 6th day. The battery is more frequently used as short-term (less than 5 h) energy storage in the fair days. It is actually empty in most of time. In addition, the size of battery is small compared to the maximum load demand. This is mainly due to the load profile characteristics for commercial building. The load peak for commercial building appears in the daytime when the PV has a larger output. Thus, most of the electricity generated by PV can be directly used by consumers and no need to be stored in the battery. Therefore, only a small battery is required for carrying the excess solar power beyond the load demand. When the solar energy cannot meet the demand of loads, the system is in turn connected to the main grid to achieve a stable operation of the hybrid system.

Fig. 7 shows the cost compositions of COE for the grid connected commercial building HES with the sizes of 3372 m^2 PV and 302 kW h battery. It has to be noted that the PV subsidies are included in the COE calculation. The simulation results show that the main grid and PV respectively provide 59.8% and 40.2% of total electricity requirement. However, as we can see from Fig. 7, the main grid costs (electricity purchase cost and emission cost) contribute over 89% of COE. PV and battery cost less than 9% of COE while they contribute up to 40.2% of total power supply.

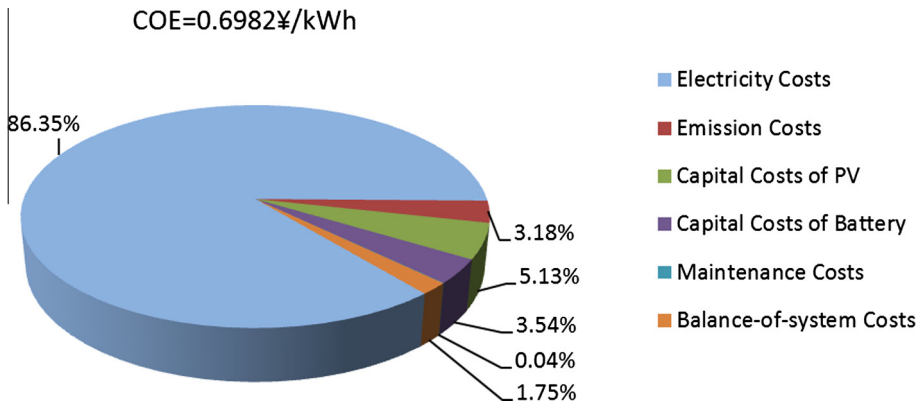

Fig. 7. Cost composition of the commercial building HES with the sizes of 3372 m^2 PV and 302 kW h battery (COE = 0.6982 ¥/kW h).

Obviously, the proposed HES for the commercial buildings can effectively reduce the electricity cost. This is due to government subsidy for PV used in the HES. Meanwhile, the characteristic of load profile for commercial building is similar to the solar radiation profile, which can minimize the capital cost of the battery for power shift.

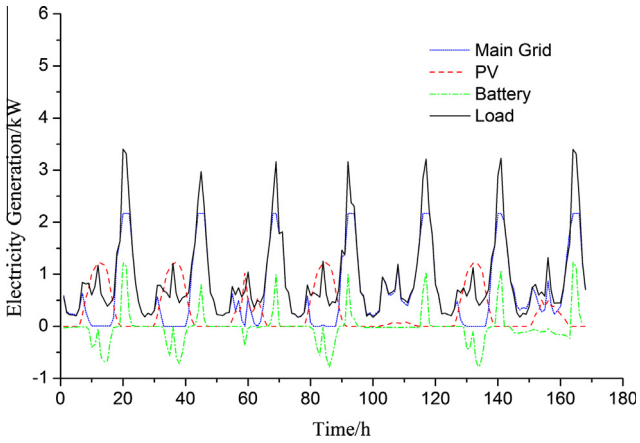

Fig. 8. Power dispatch schedule of residential building HES at the optimal-size combination (COE = 0.5459 ¥/kW h).

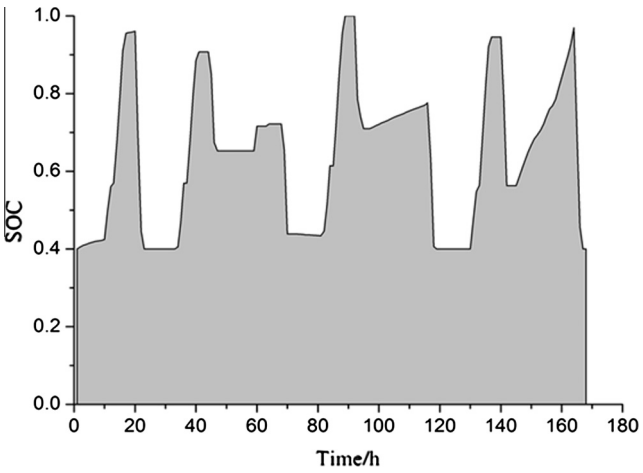

Fig. 9. Battery charging status curve of residential building HES at the optimal-size combination (COE = 0.5459 ¥/kW h).

4.3. Techno-economic performances of residential building HES

An optimal size combination for residential building HES is given as follows: 2.17 kW main grid (maximum power), 7.45 m^2 PV, and 5.16 kW h battery. In this section, the techno-economic performances of the residential building HES are based on this case.

Fig. 8 shows the power dispatch schedule of residential building HES at the lowest COE. The horizontal axis represents the time (hours) and the vertical axis represents the electricity from the HES components and the loads (kW). In this scenario, the peak power demand appears in the nighttime. The size of PV is comparative to the maximum load in the daytime. The battery shifts the PV power in daytime to the nighttime. It can be seen from Fig. 8 that the peak of power demand in the night is about 3 kW and appears at around 8: 00 PM. In the nighttime, the main grid plays the role of the primary energy source providing the power service. In Fig. 8, the charged electricity to the battery (the negative part of the green line) approximately equals to the difference between the PV curve (red line) and the load curve. This indicates that PV can provide adequate and stable electricity supply in the fair days (the 1st, 2nd, 4th and 6th day). The surpassed power from PV is stored in the battery for a later use in the night. In rainy or cloudy days, the electricity generated from PV is limited, and the main grid has to be connected during the day.

In this case, the battery is frequently used and stores part of the electricity generated during the day to meet the load demand during the night. Fig. 9 shows the SOC evolution of battery during the power dispatch of the proposed residential building HES. Compared to that of commercial building HES, the battery in the residential building HES is more effectively utilized. Within the seven simulation days, the battery has gone through 5 times of approximately full charge and discharge cycles. This is due to the significant temporal dislocation between the peak of the load profile of residential building and the peak of the solar radiation profile. The battery plays a role of eliminating the time mismatch between the generators and the consumers.

It should be noticed that the battery charge and discharge process are accompanied by energy loss. In this work, the charge and discharge efficiency of the battery are assumed to be 90%. Simulation results show that the energy loss due to the battery charge and discharge cycles accounts for 1.85% of total electricity generation for the residential building HES.

Fig. 10 shows the cost compositions of COE for the residential building HES with the sizes of 7.45 m^2 PV and 5.16 kW h battery. The simulation results show that the electricity from PV is approx-

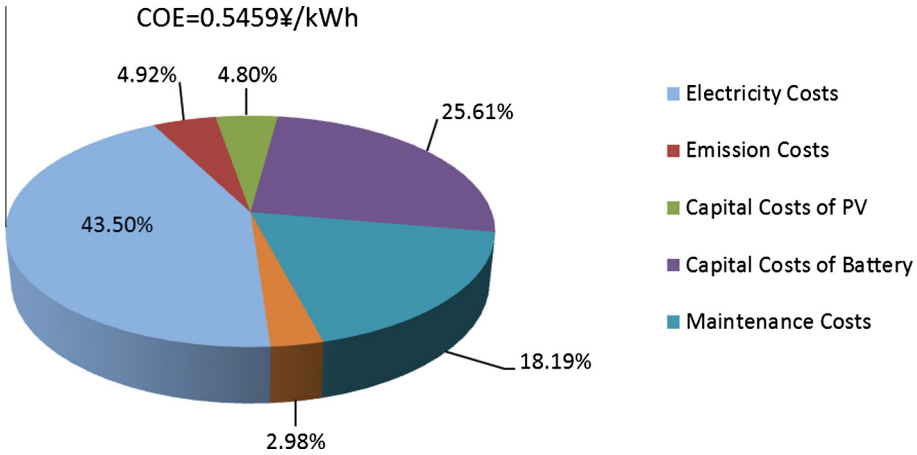

Fig. 10. Cost composition of COE for the residential building HES (excluding the main grid) with the sizes of 7.45 m^2 PV and 5.16 kW h battery (COE = 1.3697 ¥/kW h).

imately 28.9% of total power demand. The rest power supply is from the main grid. As we can see from Fig. 10, the PV capital cost only contributes 4.8% of COE while the battery capital cost accounts for up to 25.6% of total costs. This is because a larger battery capacity is required to shift the PV power from daytime to nighttime for the residential building HES. Meanwhile, the battery is used more frequently, which results in an acceleration of battery lifetime loss and therefore the increase of the replacement costs of battery.

5. Conclusions

For those commercial buildings with higher power demand in the daytime, particularly when the building load profiles have similar characteristics as the solar radiation profile, the HES with the integration of BAPV can significantly reduce the electricity bill for customers. Potentially, the use of BAPV in the case of the commercial building HES can cut COE by 46% of the commercial electricity price of the main grid. The residential buildings have lower electricity load in the daytime while its peak power demand appears in the night, which results in the requirement of a large capacity of battery and the increase of the charge-discharge cycling of battery. Therefore, the initial capital cost and replacement capital cost of battery increase significantly. The simulation results show that the COE of the residential building HES is even higher than the residential electricity price. For PV based residential HES, the lifetime and capital cost of battery have more influence on the COE than that of PV. It has to be noted that the above conclusions are only applicable under current Chinese regulatory conditions and input data.

Acknowledgement

This work was supported by National 1000 Talents Program of China, National Nature Science Foundation of China (Grant No. 51276145) and the 111 Project (Grant No. B16038).

References

[1] X. Zhang, S.H. Chan, H.K. Ho, S.C. Tan, M. Li, G. Li, et al., Towards a smart energy network: the roles of fuel/electrolysis cells and technological perspectives, Int. J. Hydrogen Energy 40 (21) (2015) 6866–6919.
[2] X. Zhang, S.C. Tan, G. Li, J. Li, Z. Feng, Components sizing of hybrid energy systems via the optimization of power dispatch simulations, Energy 52 (52) (2013) 165–172.
[3] Sandia National Laboratories, Stand-Alone Photovoltaic Systems - A Handbook of Recommended Design Practices, SAND87-7023, National Technical Information Service, U.S. Dept. of Commerce, 5285 Port Royale Road, Springfield, 1991 (VA 22161).
[4] J. Salom, J. Widén, J.A. Candanedo, I. Sartori, K. Voss, A.J. Marszal, Understanding net zero energy buildings: evaluation of load matching and grid interaction indicators, in: Conference Understanding net Zero Energy Buildings: Evaluation of Load Matching and Grid Interaction Indicators.
[5] R. Baetens, R.D. Coninck, L. Helsen, D. Saelens, The impact of load profile on the grid-interaction of building integrated photovoltaic (BIPV) systems in low-energy dwellings, J. Green Build. 5 (4) (2010) 137–147.
[6] G.C. Seeling-Hochmuth, Optimisation of hybrid energy systems sizing and operation control Dr.-Ing. Dissertation, University of Kassel, Germany, 1998 (October).
[7] C.D. Barley, C.B. Winn, Optimal dispatch strategy in remote hybrid power systems, Sol. Energy 58 (s 4-6) (1996) 165–179.
[8] C. Marnay, G. Venkataramanan, M. Stadler, A.S. Siddiqui, R. Firestone, B. Chandran, Optimal technology selection and operation of commercial-building microgrids, IEEE Trans. Power Syst. 23 (3) (2008) 975–982.
[9] T. Lambert, P. Gilman, P. Lilienthal, Chapter 15. Micropower system modeling with homer, Int. Alternat. Sources Energy (2006).
[10] RETScreen International Clean Energy Decision Support Centre, Clean Energy Project Analysis – RETScreen Engineering & Case Textbook, third ed., Minister of Natural Resources Canada,, 2005 (September).
[11] R. Dufo-López, J.L. Bernal-Agustín, Design and control strategies of PV-Diesel systems using genetic algorithms, Sol. Energy 79 (1) (2005) 33–46.
[12] G.C. Seeling-Hochmuth, A combined optimisation concet for the design and operation strategy of hybrid-PV energy systems, Sol. Energy 61 (2) (1997) 77–87.
[13] Martinez JA, de León F, Dinavahi V. Simulation tools for analysis of distribution systems with distributed resources. in: Present and Future Trends. Conference Simulation tools for Analysis of Distribution Systems with Distributed Resources. Present and Future Trends. IEEE, p. 1–7.
[14] J. Martinez-Velasco, F. de Leon, V. Dinavahi, Simulation tools for analysis and design of distribution networks with distributed energy resources, Electr. Power Qual. Utilisation J. (2009) 15.
[15] A. Chauhan, R. Saini, A review on integrated renewable energy system based power generation for stand-alone applications: configurations, storage options, sizing methodologies and control, Renew. Sustain. Energy Rev. 38 (2014) 99–120.
[16] R. Luna-Rubio, M. Trejo-Perea, D. Vargas-Vázquez, G.J. Ríos-Moreno, Optimal sizing of renewable hybrids energy systems: a review of methodologies, Sol. Energy 86 (4) (2012) 1077–1088.
[17] A. Kaabeche, M. Belhamel, R. Ibtiouen, Sizing optimization of grid-independent hybrid photovoltaic/wind power generation system, Energy 36 (2) (2011) 1214–1222.
[18] R. Jallouli, L. Krichen, Sizing, techno-economic and generation management analysis of a stand alone photovoltaic power unit including storage devices, Energy 40 (1) (2012) 196–209.
[19] C. Brandoni, M. Renzi, Optimal sizing of hybrid solar micro-CHP systems for the household sector, Appl. Therm. Eng. 75 (2015) 896–907.
[20] J.K. Kaldellis, D. Zafirakis, E. Kondili, Optimum autonomous stand-alone photovoltaic system design on the basis of energy pay-back analysis, Energy 34 (9) (2009) 1187–1198.
[21] O. Erdinc, M. Uzunoglu, Optimum design of hybrid renewable energy systems: overview of different approaches, Renew. Sustain. Energy Rev. 16 (3) (2012) 1412–1425.
[22] E. Koutroulis, D. Kolokotsa, A. Potirakis, K. Kalaitzakis, Methodology for optimal sizing of stand-alone photovoltaic/wind-generator systems using genetic algorithms, Sol. Energy 80 (9) (2006) 1072–1088.
[23] H. Yang, W. Zhou, L. Lu, Z. Fang, Optimal sizing method for stand-alone hybrid solar–wind system with LPSP technology by using genetic algorithm, Sol. Energy 82 (4) (2008) 354–367.
[24] H. Li, R. Nalim, P.A. Haldi, Thermal-economic optimization of a distributed multi-generation energy system – a case study of Beijing, Appl. Therm. Eng. 26 (7) (2006) 709–719.
[25] F. Ascione, N. Bianco, R.F. De Masi, C. De Stasio, G.M. Mauro, G.P. Vanoli, Multi-objective optimization of the renewable energy mix for a building, Appl. Therm. Eng. (2015).
[26] R. Bornatico, M. Pfeiffer, A. Witzig, L. Guzzella, Optimal sizing of a solar thermal building installation using particle swarm optimization, Energy 41 (1) (2012) 31–37.
[27] A.K. Kaviani, G.H. Riahy, S.M. Kouhsari, Optimal design of a reliable hydrogen-based stand-alone wind/PV generating system, considering component outages, Renewable Energy 34 (11) (2009) 2380–2390.
[28] S. Ghaem Sigarchian, M.S. Orosz, H.F. Hemond, A. Malmquist, Optimum design of a hybrid PV–CSP–LPG microgrid with Particle Swarm Optimization technique, Appl. Therm. Eng. (2016).
[29] R.S. Garcia, D. Weisser, A wind–diesel system with hydrogen storage: joint optimisation of design and dispatch, Renewable Energy 31 (14) (2006) 2296–2320.
[30] Y. Shin, W.Y. Koo, T.H. Kim, S. Jung, H. Kim, Capacity design and operation planning of a hybrid PV–wind–battery–diesel power generation system in the case of Deokjeok Island, Appl. Therm. Eng. 89 (2015) 514–525.
[31] F. Nicolin, V. Verda, Lifetime optimization of a molten carbonate fuel cell power system coupled with hydrogen production, Energy 36 (36) (2011) 2235–2241.
[32] A. Mellit, Sizing of a stand-alone photovoltaic system based on neural networks and genetic algorithms: application for remote areas, Istanbul Univ. – J. Electr. Electron. Eng. 7 (2) (2007).
[33] J. Lagorse, D. Paire, A. Miraoui, Sizing optimization of a stand-alone street lighting system powered by a hybrid system using fuel cell, PV and battery, Renew. Energy 34 (3) (2009) 683–691.
[34] S. Kamel, C. Dahl, The economics of hybrid power systems for sustainable desert agriculture in Egypt, Energy 30 (8) (2005) 1271–1281.
[35] A.R. Prasad, E. Natarajan, Optimization of integrated photovoltaic–wind power generation systems with battery storage, Energy 31 (12) (2006) 1943–1954.
[36] W. Zhou, H. Yang, Z. Fang, Battery behavior prediction and battery working states analysis of a hybrid solar–wind power generation system, Renewable Energy 33 (6) (2008) 1413–1423.
[37] I.F. Roth, L.L. Ambs, Incorporating externalities into a full cost approach to electric power generation life-cycle costing, Energy 29 (s 12-15) (2004) 2125–2144.
[38] H. Kang, Economic Optimization of Cool & Heat Cogeneration System Based on Differential Evolution Algorithm, Xi'an Jiaotong University, Xi'an, 2008 (in Chinese).
[39] K. Renguan, Research on Typical Power Supply Mode of Microgrid and Optimal Allocation of Micropower, Zhejiang University, Hangzhou, 2013 (in Chinese).
[40] N. Fall, L. Giles, Marchionini B, et al. Remote Area Power Supply (RAPS) Load and Resource Profiles[EB.OL], 2007. [2015-1-25]. <http://prod.sandia.gov/techlib/access-control.cgi/2007/074268.pdf>.
[41] X. Zhang, A statistical approach for sub-hourly solar radiation reconstruction, Renewable Energy 71 (71) (2014) 307–314.
[42] H. Tsuchiya, O. Kobayashi, Mass production cost of PEM fuel cell by learning curve, Int. J. Hydrogen Energy 29 (10) (2004) 985–990.

[43] L. Ren, Y. Zhu, J. Jin, F. Cheng, Proton exchange membrane fuel cell for electric vehicle, Battery Bimonthly 31 (5) (2001) 251–253 (in Chinese).
[44] Price Bureau of Xi'an, Notice on Standardizing the Way of Marking Price for Property Services Related Charges. 24 April, 2013, (in Chinese) <http://www.12358.gov.cn/websac/cat/634444.html>.
[45] State Counci. Notice on issuing the Second Five-Year plan about energy saving. 6 August, 2012 (In Chinese), <http://www.gov.cn/xxgk/pub/govpublic/mrlm/201208/t20120821_65505.html>.
[46] Emission factors of air pollutants and CO_2 from the combustion of Chinese fossil fuels (2000). Report of China top 100 coal enterprises, 2005 (in Chinese).
[47] National Development and Reform Commission (NDRC) of China; National PV Power Plant Benchmark Feed-in Tariffs Table; 26 August, 2013 (in Chinese), <http://www.sdpc.gov.cn/zcfb/zcfbtz/201308/W020130830538568620813.pdf>.